Published in Image Processing On Line on 2023–06–28.
Submitted on 2021–11–25, accepted on 2022–10–19.
ISSN 2105–1232 © 2023 IPOL & the authors CC–BY–NC–SA
This article is available online with supplementary materials,
software, datasets and online demo at
https://doi.org/10.5201/ipol.2023.389

A Data Set for Fall Detection with Smart Floor Sensors

Charles Truong[1⋆], Mounir Atiq[1⋆], Ludovic Minvielle[1], Renan Serra[2], Mathilde Mougeot[1,3], Nicolas Vayatis[1]

[1] Université Paris-Saclay, ENS Paris-Saclay, CNRS, Centre Borelli, Gif-sur-Yvette, France
[2] Tarkett GDL S.A., Luxembourg
[3] ENSIIE, Evry, France
⋆ Contributed equally

Communicated by Laurent Oudre *Demo edited by* Charles Truong

Abstract

This article describes a data set of falls and activities of daily living recorded with a pressure floor sensor. These signals have been recorded under two settings, one constrained – with volunteers following a predefined protocol, and one unconstrained – where data were collected in a partner nursing home. Overall 157 hours of signal are made available along with 563 manually annotated falls and 333 manually annotated activities (e.g. running, walking). For ease of use, code snippets and an online interface are also provided.

Source Code

The data described in this article can be downloaded from the associated web page[1]. Code snippets to load and manipulate the signals and the associated metadata can be found at the article web page and also online[2].

Keywords: biomedical data set; fall detection; classification; multivariate time series

1 Introduction

Falls present a major risk for the elderly people health and independence. It has been shown that more than 30% of individuals above 65 years old fall at least once a year, and that the worldwide elderly population is growing faster than any other age group [1]. While relatively unharmful to a young healthy person, a fall, when happening to an elderly individual, may lead to serious injury and even death [2]. Moreover 10% to 25% of falls in elderly care institutions result in fracture or laceration and their consequences are not only physical (articular frailty, head injuries) but also psychological (fear of falling, diminishing social life), thus increasing the level of dependence and therefore the risk

[1] https://doi.org/10.5201/ipol.2023.389
[2] https://github.com/deepcharles/fall-data

of falling again [24]. Besides, research shows that after a fall, the time a person spends on the floor is critical. Indeed, nearly one person in two needs assistance to get up, and a "long lie" can lead to serious complications (hypothermia, dehydration) and an increased frailty [12]. In this context, monitoring systems and robust algorithms for automatic fall detection have received a lot of attention in the last twenty years, resulting in a vast and varied literature [8, 30, 22]. Compared to the number of published articles, the number of open and curated data sets is quite low. Indeed such data are hard to gather, involve sensitive information and require a lot of manpower to label. Nevertheless, in the field of fall detection, as well as in other applied domains [28], data from real-world situations with expert labels are necessary and useful contributions for the design and objective comparison of better detection methods.

Available data sets generally come from either wearable sensors or video-based monitoring systems, or a combination of both. Wearable sensors, typically accelerometers and gyroscopes, are arguably the cheapest and easiest to install fall detection systems. Data are produced by a single dedicated Inertial Measurement Unit (IMU) fixed to the patient's body [10], or from several synchronized units [25, 5, 27]. The IMU can also be replaced by a simple smartphone [16, 7], sometimes combined with a smartwatch [29] or force sensors integrated in "smartshoes" [18]. Nevertheless, when dealing with elderly daily activity monitoring, such sensors suffer from one main drawback: patients may forget to wear those devices or even refuse to wear them, as they can be regarded as intrusive. Compared to wearable sensors, video cameras are ambient sensors that require no action from the patients. They are also able to record a large amount of information, thus allowing the extraction of more complex features for additional monitoring tasks. Video-based data sets include streams from a classical RGB camera [6], or from a depth camera (usually a Microsoft Kinect) [3, 15, 13]. To improve detection accuracy, several cameras can be combined [4, 31], and wearable sensors can be synchronized with the video feed [20, 11, 14]. However, these systems are likely to raise privacy concerns, and, depending on the area's organization, they can face occlusion or coverage issues. Table 1 summarizes the available data sets for the fall detection task.

Compared to the available corpus of open data sets, our proposal stems from a quite different monitoring system. It consists in a "smartfloor" equipped with floor pressure sensors (based on a piezoelectric material) that can deal with areas of arbitrary size without any coverage or occlusion issues. This approach does not interfere with the daily habits of monitored patients, and addresses the privacy issue of other systems, at the expense of a more cumbersome installation. Overall 157 hours of signal are made available along with 563 manually annotated falls and 333 manually annotated non-fall activities (e.g. walking, running). The data are divided in three parts: (i) a controlled setting where falls were simulated by healthy volunteers ($\sim 70\%$ of the falls), (ii) a controlled setting where healthy volunteers performed non-fall activities, and (iii) an unconstrained setting, with actual falls ($\sim 30\%$ of the falls) from elderly patients in a partner nursing home. In addition to the data, code snippets[3] and an online interface are provided, for ease of use. Note that part of this data set has been used in [17, 19].

2 Acquisition

This section describes the acquisition system used to detect falls and the data collection protocol.

2.1 Equipment

Data were collected with floor sensors designed by Tarkett (`www.tarkett.fr`), a French flooring company, as part of their effort to create "smartfloors" to deploy in various medical and industrial

[3] `https://github.com/deepcharles/fall-data`

Article	Size	Sensor	Simulated falls	Real falls	Other activities
[10]	16 subjects, 270 minutes in total	Single IMU	Yes	No	Yes
[25]	15 subjects, 26 420 acquisitions of about 20s each	Several IMUs	Yes	No	Yes
[5]	17 subjects, 531 acquisitions of about 15s	Several IMUs	Yes	No	Yes
[27]	38 subjects, 4510 acquisitions from 10s to 100s	Two IMUs	Yes	No	Yes
[16]	10 subjects, around 1700 acquisitions	One or two smartphones	Yes	No	Yes
[7]	66 subjects, around 3200 acquisitions	Single smartphone	Yes	No	Yes
[29]	3 subjects	Smartwatch + smartphone	Yes	No	Yes
[18]	17 subjects, 680 acquisitions	"Smartshoes"	Yes	No	Yes
[6]	9 subjects, 191 videos	Single camera	Yes	No	Yes
[3]	5 subjects	Kinect camera	Yes	No	Yes
[15]	184 videos	Kinect camera	Yes	No	Yes
[13]	10 subjects, 1800 videos	Kinect camera	Yes	No	Yes
[4]	24 acquisitions	8 cameras	Yes	No	Yes
[31]	5 subjects, 180 videos	2 Kinect cameras	Yes	No	Yes
[20]	12 subjects, 82 minutes of acquisition	Motion capture, 4 cameras, 2 Kinect cameras, accelerometers, microphones	Yes	No	Yes
[11]	70 acquisitions	2 Kinect cameras + IMU	Yes	No	Yes
[14]	17 subjects, 33 acquisitions	5 IMUs + EEG + infrared sensors + 2 cameras	Yes	No	Yes
Our article	563 acquisitions	Floor pressure sensors	Yes	Yes	Yes (without label)

Table 1: Summary of available data sets for the fall detection task. Other activities labeled in those data sets include walking, jumping, sitting, etc. Note that our data set is the only one containing real falls.

settings. It consists of piezolectric sensors embedded into the flooring and a processing unit.

Piezoelectric sensors. The sensor used by Tarkett's system is composed by an electro-mechanical electret, namely EMFi or EMFit, that has a piezoelectric property [21]. When stressed or squeezed, a *piezoelectric* material (not to be confused with a *piezoresistive* material) emits charges, causing a change in the electric potential. Figure 1 illustrates the principle behind a piezoelectric floor sensor. Roughly speaking, the charge Q and the force F received by the material are linked as follows: $Q = d \times F$, where $d \simeq 234pC \cdot N^{-1}$ is the piezoelectric coefficient, also known as sensitivity. So this sensor does not need any power supply to generate its output, however the amplitude of the produced electric charge signals is very low (under the range of $1\mu C$). For this reason an external electronic amplification circuit is necessary to process the signal. It is comparable to a capacitor (with a capacitance density of $22pF \cdot cm^{-2}$ [26]), where pressure forces variation rule the charge and discharge of the capacitor. Tarkett's system takes advantage of this property, and the piezoelectric material acts as a dynamic pressure sensor: by applying a constant force, a user will see the output signal increase then return to its initial value. This sensor relaxation phenomenon follows

an exponential function with a fixed parameter determined by the total capacitance of the sensor and the components of the electronic amplification circuit. Moreover the more the charge displacement is important compared to the total capacitance the more the produced signal is accurate. For this reason, using smaller surfaces, the same sensor has been used in other applications on cardiac or respiratory activity [23, 9].

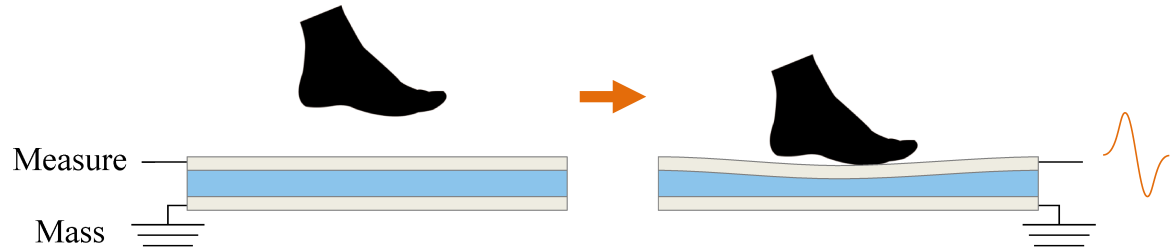

Figure 1: Piezoelectric sensor principle. When deformed, the piezoelectric material emits charges, hence a transient current can be measured as output.

Equipment setup. The sensor comes in 60 cm wide bands and is placed directly under the flooring. The bands are initially rolls of about 100 meters that can be cut every 30 cm. Once cut, bands can be linked together with small flat connectors to cover an area. Any output signal that is produced is sent to a processing unit. A sensor band with its connector is pictured in Figure 2 and a schematic view of the sensor and its setup is shown in Figure 3. This system could work with any type of flooring but, as the signal amplitude is proportional to the sensor's deformation, the more the flooring absorbs pressure the less the signal is accurate. In real conditions, equipped rooms share the same characteristics : the flooring, the total size (between 15 and 30 m^2) and three distinct sensor areas that are the entrance, the bathroom and the bedroom. The processing unit has 8 entry channels, allowing each unit to process a large surface covered by connected bands. However Tarkett mainly uses 3 of these entries for each of the described areas, which restricts importantly the spatial information that can be extracted. The processing unit is designed to handle the signal from end to end (from basic filtering to event detection) and to communicate with servers (sending signal recordings) and the nursing home (sending information such as activity reports or alarms). When it reaches the unit, the signal is first passed through an analog charge amplifier that converts the charge signal into voltage (between 0V and 3.3V), and is then converted linearly, through an ADC (Analog-Digital Converter) into a 12-bit numerical time series (between 0 and 4096) sampled at a frequency of 100 Hz. The unit is equipped with a 32-bit 500 MHz processor, accompanied with 256 MB of RAM, and 500 MB of local storage. The signal from each band of sensors is individually preprocessed (low-pass filter and offset correction) before begin recorded. Articles that have used this data set for fall detection did not apply any additional filtering.

2.2 Protocol

A number of signals were recorded and labeled in a partner nursing home, with actual residents, caregivers and visitors going about their everyday activities. In unconstrained as well as controlled setting the type of flooring on top of the sensor is the same, but the sensitivity d can vary (up to 10%). Collection and labeling in such an unconstrained setting are costly processes. This is the reason why the data set was augmented with signals recorded in a controlled setting, with healthy volunteers simulating falls as well as other real-life events. Both settings are now described.

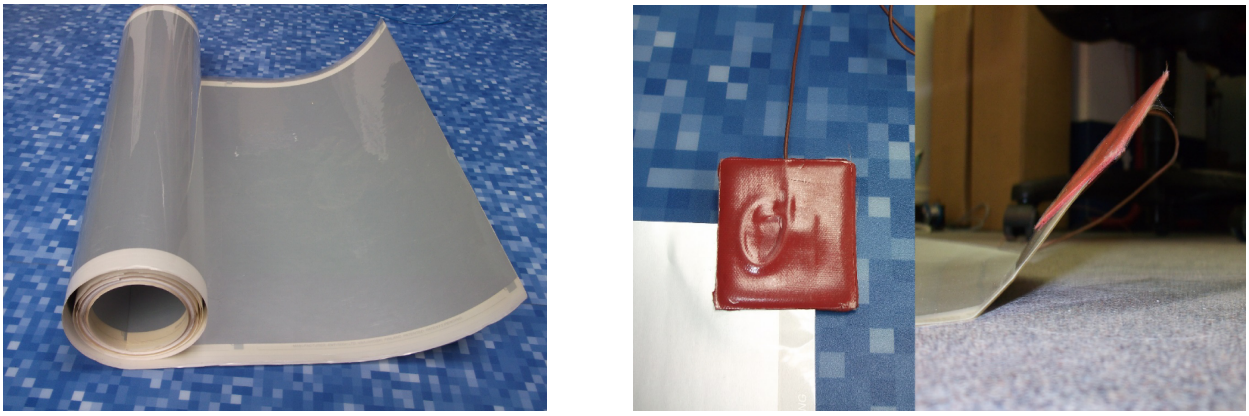

(a) Roll of sensor (b) Connector

Figure 2: Photographs of a roll of sensor and a connector.

(a) Sensor cross-sectional view (b) Fall detection system

Figure 3: (a) Sensor view. A roll of sensor can be installed directly onto the concrete and covered by the flooring. (b) In this installation example, there are three areas (bathroom, bedroom and entrance) and all signals are sent to a processing unit.

Controlled setting. A pilot site was equipped with Tarkett's system to reproduce a basic room setup with 3 areas, illustrated in Figure 3 and all the controlled acquisitions come from this unique installation. Data have been generated by 28 healthy volunteers who were asked to fall, on several occasions and in different areas, resulting in 742 signals collected from the floor sensors. In each trial, a single fall is recorded, or a non-fall activity, to better simulate real-life settings.

Several types of fall were imitated in this controlled setting. Falls are categorized by their starting positions and direction of fall; this data set includes the six following types: sitting on a chair and falling backward or sideward, standing and falling forward, backward, sideward or vertically. In the following, those fall types are respectively denoted "BackwardFromChair", "SidewardFromChair", "ForwardFromStanding", "BackwardFromStanding", "SidewardFromStanding", "VerticallyFromStanding". After each fall, all participants remained still for a few seconds on the floor, before getting up. All acquisitions were simultaneously video-recorded for labelling. The distribution of fall types is shown in Table 2. In the controlled setting, data were collected between May 2014 and February 2015.

Controlled setting without fall. Several non-fall activities were also recorded with the smart floor sensors. They include common daily actions such as walking a few steps (labeled as "Walk" in the metadata, see Section 3.2), running ("Run"), jumping ("Jump"), interactions with objects, e.g. sitting down on a chair ("ObjectInteraction"), letting an object fall then picking it up ("ObjectFalling"). For "Walk" and "Jump", on some occasions, multiple people were simultaneously on the floor sensors; this is indicated by a flag "MultiplePeople" which can be "true" or "false" in the metadata. Also, for "Walk", recorded subjects sometimes used a walking aid: a walking frame with wheels ("WalkerWheels") or without wheels ("WalkerFoot"), a walking stick ("WalkingStick") or a

Setting	Fall type	Number of signals	Average duration	Average duration of fall event
Controlled	ForwardFromStanding	122	18.89 s	1.24 s
	SidewardFromStanding	113	18.96 s	1.06 s
	BackwardFromStanding	102	20.27 s	1.28 s
	VerticallyFromStanding	44	22.77 s	1.33 s
	BackwardFromChair	11	16.73 s	1.15 s
	SidewardFromChair	17	17.71 s	0.97 s
	Total	409	19.56 s	1.19 s
Unconstrained	N/C	154	3569.47 s (59.5 min)	N/C

Table 2: Types of fall for the 563 signals from the "Controlled" and "Unconstrained" settings. "N/C" stands for "Not communicated".

Setting	ActivityType	MultiplePeople	WalkingDevice	Number of signals	Average duration
ControlledNoFall	Jump	False	None	10	15.9 s
		True	None	4	25.0 s
	ObjectFalling	False	None	17	7.0 s
	ObjectInteraction	False	None	34	11.6
	Run	False	None	6	12.0
	Walk	False	None	65	14.6 s
			WalkerFoot	26	46.3 s
			WalkerWheels	30	42.9 s
			WalkingStick	28	30.7 s
			WheelChair	41	36.0 s
		True	None	50	20.7 s
			WalkingStick	22	37.1 s
Total				333	25.3 s

Table 3: Types of activities and walking aids for the 333 signals from the "ControlledNoFall" setting.

wheelchair ("WheelChair"), or nothing ("None"). Table 3 summarizes the distributions of activities across the data set. Those data were collected between May 2014 and February 2015.

Unconstrained setting. Tarkett's floor sensor system was installed in individual bedrooms in a partner nursing home (see Figure 3-b for a schematic installation). The collected signals were split in periods of approximately one hour and studied with a Tarkett algorithmic and visualization tool to find fall events. The detection method relied on the signal shape ("what pattern in the signal is the most likely to represent the flagged fall?"), the activity that followed (nurse check and call) and information from the caregivers. This data set only contains falls that were detected with a high level of certainty by an expert; other falls that were not as certain are not present. Note that falls occurred in different areas of the monitored bedrooms. This resulted in 154 signals, each containing a single fall. In addition to the falls, a wide range of daily activities from elderly people, caregivers and visitors were also recorded (but not labeled). Contrary to the controlled setting, only the timestamps of the falls are given. Each unconstrained setting signal corresponds approximately to a record of one hour duration. Provided falls timestamps are ensured to be inside the fall event but precise event start and end, as well as the fall time length, are unknown. In the unconstrained setting, data were collected between March 2017 and February 2018.

3 Data Description

All signals, either from the controlled or the unconstrained settings, consist of a `.csv` file containing the actual time series, and a `.json` file containing contextual data, which are both described in this section.

3.1 Time Series

As previously mentioned in Section 2.1, the provided time series measure the voltage of the piezoelectric sensors. After conversion by the processing unit, the signals are integer-valued (between 0 and 4096), sampled at 100 Hz and have eight dimensions (one for each entry channel of the unit). Recall that each entry channel is connected to a few rolls of sensor which cover a specific area. A person will only stand on one or (at the border between) two of those areas at any given moment. This is the reason why, most times, only one or two dimensions are active. (This is not true however when several people are present.) Representative examples are shown in Figure 4 (controlled setting), Figure 5 (controlled setting without fall) and Figure 6 (unconstrained setting). Notice, for the controlled setting and unconstrained setting, how the fall is only visible on one dimension: the sixth dimension on Figure 4 and the first dimension on Figure 6; for the latter, a close-up is shown in Figure 7. For both the controlled setting and the unconstrained settings, falls occurred in different areas of the monitored surface; as a result, the dimension activated by the fall is not the same for all acquisitions. In addition to the fall, movement is often visible: it is the result of (simulated or real-life) activities of the participants. In the controlled setting without fall, a number of activities have been recorded. On Figure 5, the activity is "Run"; similarly to the fall, it is visible on several dimensions but not all, meaning that the subject only activated a subset of the eight sensors. On average, signals last 19.56 s in the controlled setting and a fall lasts 1.19 s. In the controlled setting without fall, a signal lasts 25.3 s on average. In the unconstrained setting, time series last almost one hour on average while the fall duration is not communicated. In all settings, a certain level of electronic noise is always present. Those observations are summarized in Table 2 and Table 3.

3.2 Metadata

A number of contextual data are provided with each signal and are now listed. In the following, "N/C" denotes "Not Communicated".

- **Setting.** Equal to "Controlled", "Unconstrained" or "ControlledNoFall".
- **Code.** Unique identifier for the trial. It consists of one or three letters ("c" for "Controlled", "cnf" for "ControlledNoFall" and "u" for "Unconstrained") and a number, e.g. "c-24".
- **FallEventStart.** Start *index* of the fall event. It is set to "N/C" whenever **Setting** is equal to "Unconstrained" or "ControlledNoFall".
- **FallEventEnd.** End *index* of the fall event. It is set to "N/C" whenever **Setting** is equal to "Unconstrained" or "ControlledNoFall".
- **FallEvent.** *Index* of the fall event, as provided by the expert (when **Setting** is equal to "Unconstrained") or simply equal to (**FallEventStart** + **FallEventEnd**)/2 (when **Setting** is equal to "Controlled"). It is "N/C" otherwise.
- **TypeOfFall.** This variable takes value in {"ForwardFromStanding", "BackwardFromStanding", "SidewardFromStanding", "VerticallyFromStanding", "BackwardFromChair", "SidewardFromChair"}

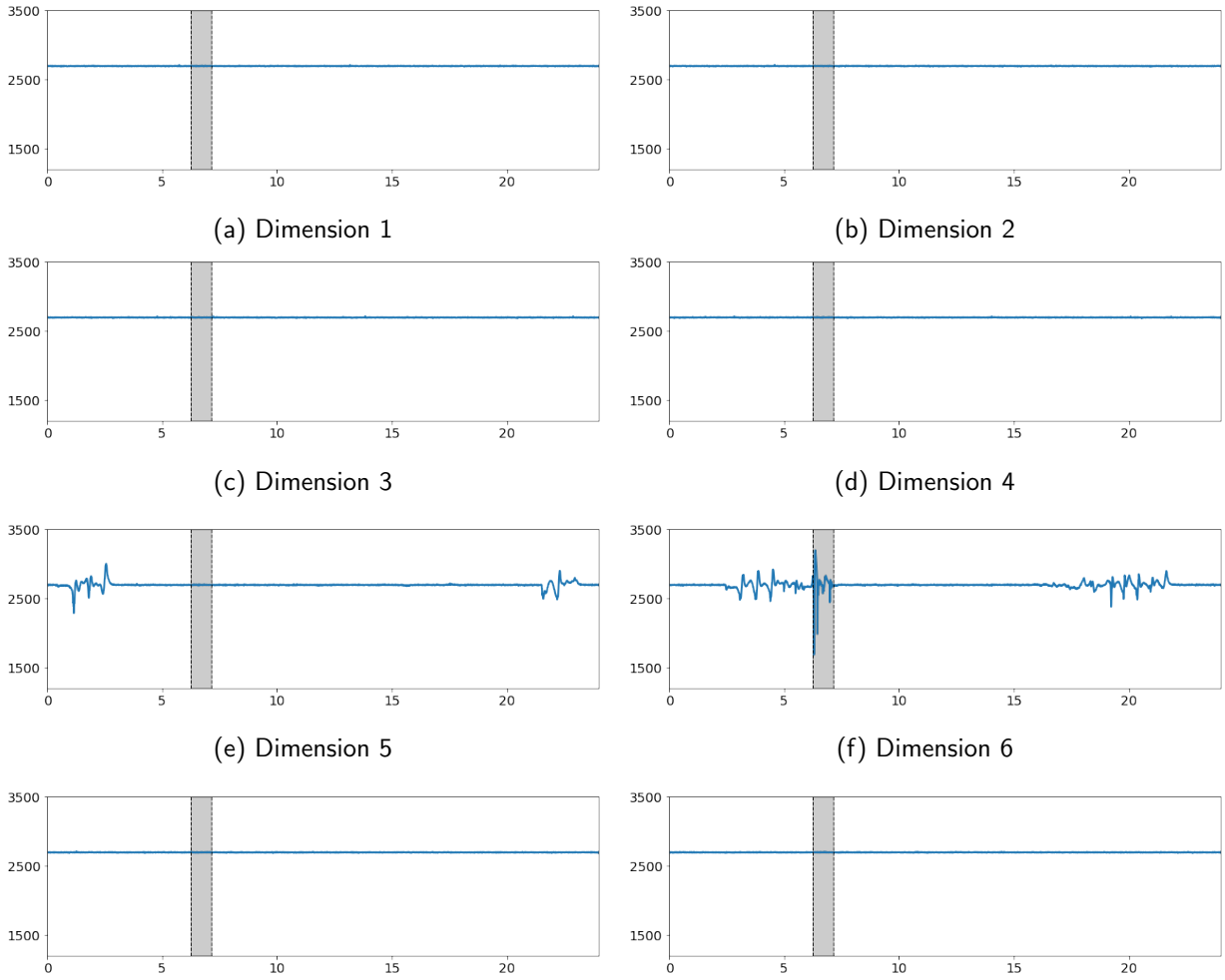

(a) Dimension 1 (b) Dimension 2

(c) Dimension 3 (d) Dimension 4

(e) Dimension 5 (f) Dimension 6

(g) Dimension 7 (h) Dimension 8

Figure 4: Signal example (controlled setting). The fall event is highlighted in grey. Time is in second (s).

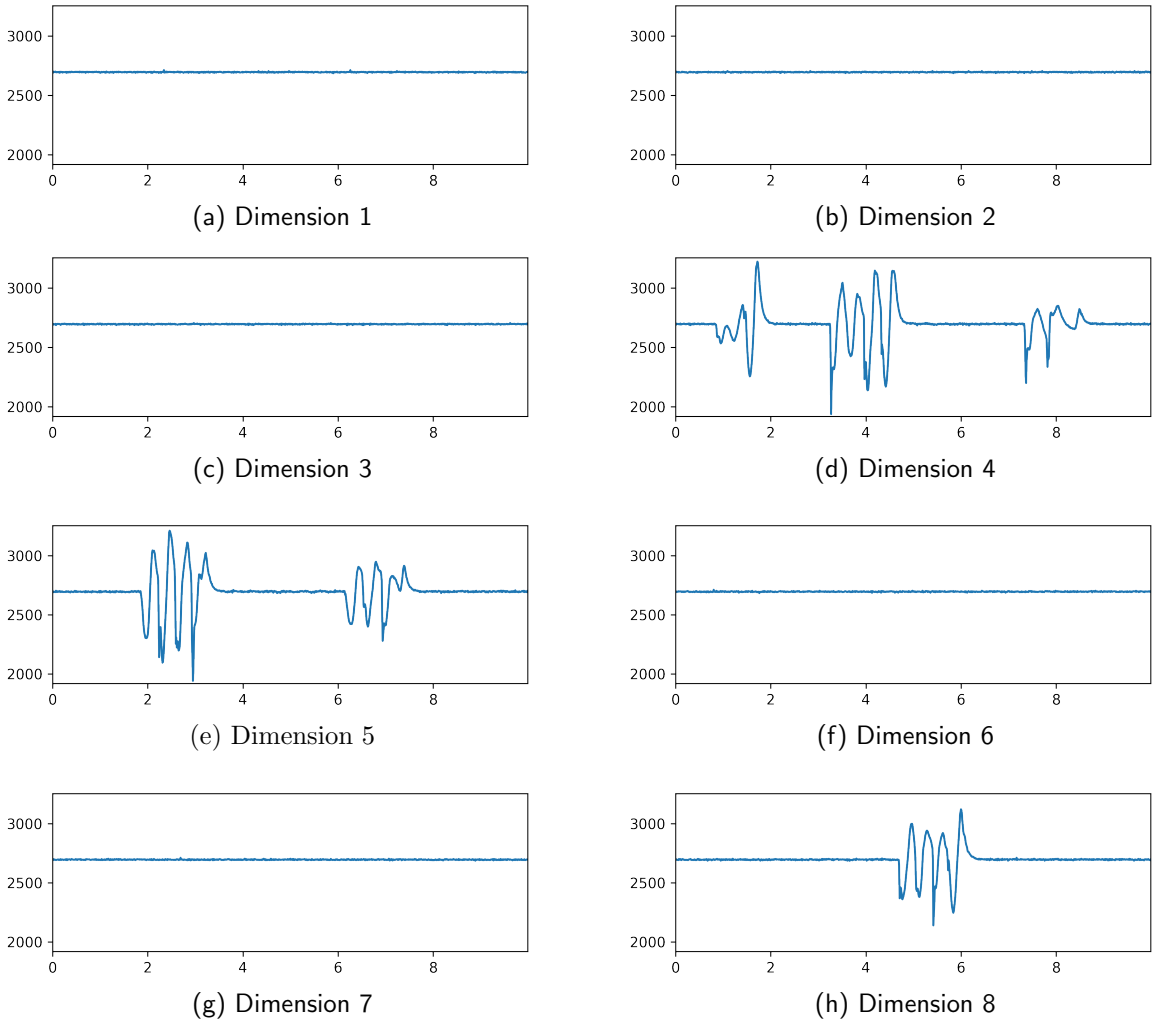

(a) Dimension 1 (b) Dimension 2

(c) Dimension 3 (d) Dimension 4

(e) Dimension 5 (f) Dimension 6

(g) Dimension 7 (h) Dimension 8

Figure 5: Signal example (controlled setting, without fall). The activity is "Run" without walking aid by a single subject. Time is in second (s).

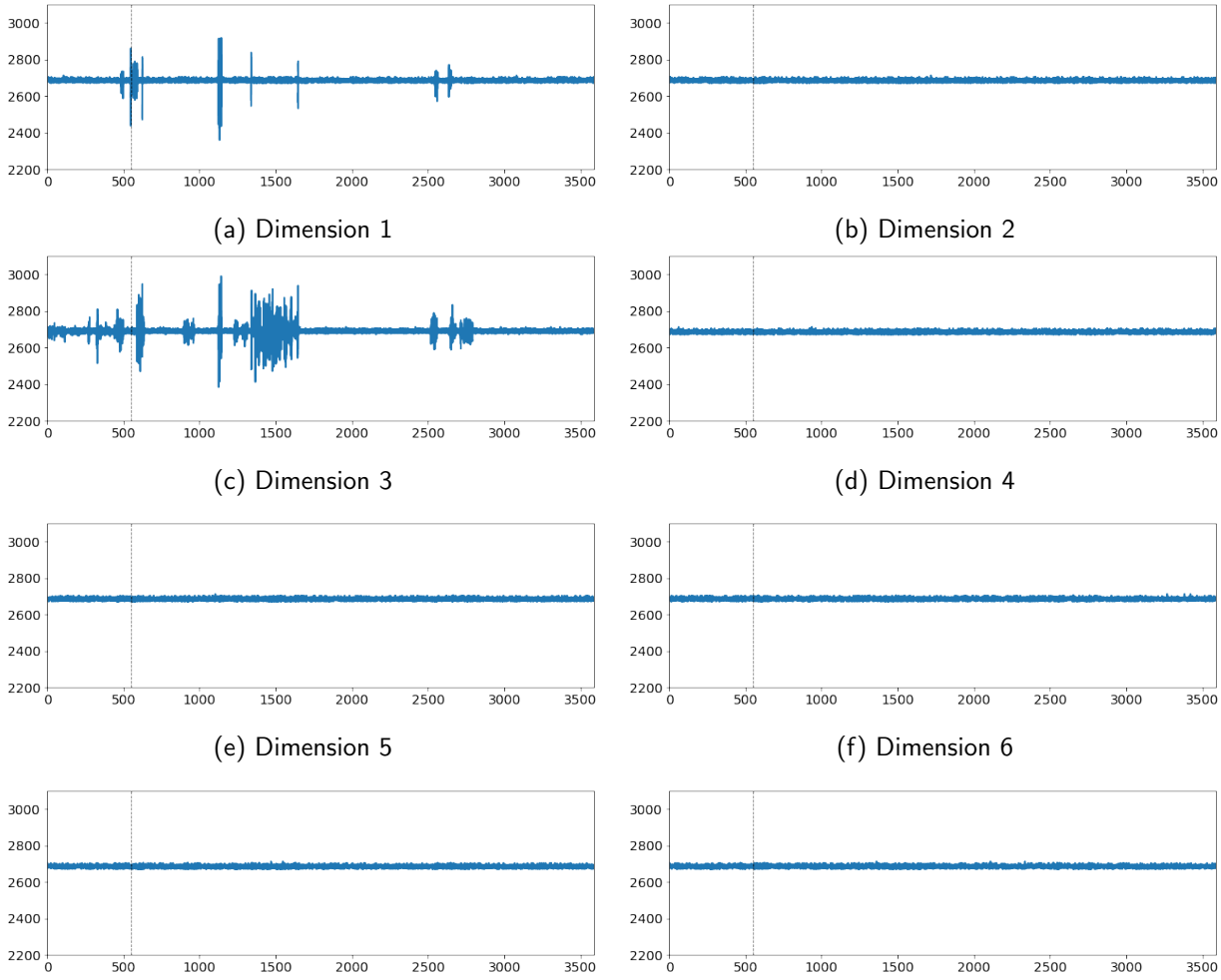

(a) Dimension 1 (b) Dimension 2

(c) Dimension 3 (d) Dimension 4

(e) Dimension 5 (f) Dimension 6

(g) Dimension 7 (h) Dimension 8

Figure 6: Signal example (unconstrained setting). The fall event is indicated by the vertical dashed line. Contrary to the controlled setting, the start and end of the event are not provided. Time is in second (s). Activities outside the annotated fall (visible on Dimensions 1 and 3) correspond to daily activities (e.g. walking, sitting down/up) by the monitored subject and possibly caretakers and visitors.

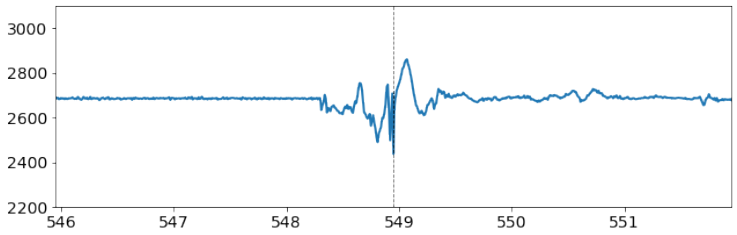

Figure 7: Close-up on the fall event of the signal example displayed in Figure 6 (dimension 1 only). The fall event is indicated by the vertical dashed line. Time is in second (s).

when **Setting** is equal to "Controlled" (see Section 2.2 for an explanation on each label), or is equal to "N/C" when **Setting** is equal to "Unconstrained" or "ControlledNoFall".

- **Length.** Time length (in seconds) of the signal.
- **ActivityType.** This variable takes value in {"Walk", "ObjectInteraction", "ObjectFalling", "Jump", "Run"} if **Setting** is "ConstrainedNoFall", and "N/C" otherwise.
- **WalkingDevice.** The type of walking aid used by the subject. It takes value in {"None", "WalkerWheels", "WalkerFoot", "WheelChair", "WalkingStick"} if **Setting** is "ConstrainedNoFall", and "N/C" otherwise.
- **MultiplePeople.** This variable indicates if there were multiple people during the recording. It is equal to "true" or "false" when **Setting** is equal to "ConstrainedNoFall", and "N/C" otherwise.

3.3 Data Format and Availability

Data are distributed in well-known data structures, namely Comma-Separated Values (CSV) and JavaScript Object Notation (JSON). In detail, each signal is associated with two files. The first one has a `.csv` extension and contains the time series. The second one has a `.json` extension and contains the metadata. Files are identified by the **Code** variable which uniquely determines a signal. For instance, the signal number 2 in the unconstrained setting is associated with the two following files: `u-2.csv` and `u-2.json`. As a result, the complete data set has 1792 files, equally distributed in `.csv` and `.json` files. A signal file (ending in `.csv`) has $D = 8$ columns and the data type is integer. A metadata file contains the names and values of the metadata described in Section 3.2 and follows the JSON format[4]. Excerpts of such files are displayed in Figure 8. The size of the archive containing the data is 339.1 MB (compressed, `.tar.gz` format) or 2.27 GB (raw format).

3.4 Data Availability

This data set is distributed under a Creative Commons CC-BY-NC-SA license[5].

4 Conclusion

In this article, 896 time series were described, collected from simulated falls and activities by volunteers with no known medical impairment, as well as actual residents from a partner nursing home.

[4] https://www.json.org
[5] https://creativecommons.org/licenses/by-nc-sa/3.0/

```
2668,2665,2667,2665,2661,2665,2662,2664
2661,2666,2655,2666,2665,2665,2666,2662
2661,2667,2668,2664,2660,2665,2671,2664
2662,2668,2670,2669,2664,2669,2670,2666
2667,2664,2667,2665,2662,2668,2663,2669
...
```

(a) Signal file

```
{
    "Code": "c-1",
    "FallEvent": 1084,
    "FallEventEnd": 1143,
    "FallEventStart": 1025,
    "Length": 27.0,
    "Setting": "Controlled",
    "TypeOfFall": "VerticallyFromStanding",
    "MultiplePeople": "N/C",
    "ActivityType": "N/C",
    "WalkingDevice": "N/C"
}
```

(b) Metadata file

Figure 8: Excerpts from a signal file (ending in .csv) and a metadata file (ending in .json)

Overall, 157 hour of signals can be downloaded, along with fall labels (start and end of fall, or only the fall timestamp). In total, 563 falls were manually annotated by experts as well as 333 non-fall activities. This data set can be used to design and compare the performance of algorithmic procedures, fall detection methods for instance. The data are made available under a CC-BY-NC-SA license, in universal file formats (JSON and CSV). Code snippets to access, visualize and perform basic analysis are available online[6][7] for several standard programming languages.

Acknowledgment

Mounir Atiq and Charles Truong are funded by the Industrial Data Analytics and Machine Learning (IDAML) chair of ENS Paris-Saclay.

Image Credits

The images in Figure 2 were obtained by the members of the Centre Borelli lab, CC-BY.

References

[1] *WHO Global Report on Falls Prevention in Older Age*, Technical Report, World Health Organization, 2007. https://digitallibrary.un.org/record/628832.

[2] *Fatal Injury Data*, Technical Report, Centers for Disease Control and Prevention, Injury Center, Injury Prevention & Control, 2018. Web-based Injury Statistics Query and Reporting System (WISQARS) https://www.cdc.gov/injury/wisqars/index.html.

[3] K. Adhikari, H. Bouchachia, and H. Nait-Charif, *Activity Recognition for Indoor Fall Detection Using Convolutional Neural Network*, in IAPR International Conference on Machine Vision Applications (MVA), 2017, pp. 81–84, https://doi.org/10.23919/MVA.2017.7986795.

[6] https://doi.org/10.5201/ipol.2023.389
[7] https://github.com/deepcharles/fall-data

[4] E. Auvinet, C. Rougier, J. Meunier, A. St-Arnaud, and J. Rousseau, *Multiple Cameras Fall Dataset*, Dataset, University of Montréal, 2010. http://www-labs.iro.umontreal.ca/~labimage/Dataset/.

[5] E. Casilari, J. A. Santoyo-Ramón, and J. M. Cano-García, *UMAFall: A Multisensor Dataset for the Research on Automatic Fall Detection*, Procedia Computer Science, 110 (2017), pp. 32–39, https://doi.org/10.1016/j.procs.2017.06.110.

[6] I. Charfi, J. Miteran, J. Dubois, M. Atri, and R. Tourki, *Optimized Spatio-Temporal Descriptors for Real-Time Fall Detection: Comparison of Support Vector Machine and Adaboost-Based Classification*, Journal of Electronic Imaging (JEI), 22 (2013), p. 17, https://doi.org/10.1117/1.JEI.22.4.041106.

[7] C. Chatzaki, M. Pediaditis, G. Vavoulas, and M. Tsiknakis, *Human Daily Activity and Fall Recognition Using a Smartphone's Acceleration Sensor*, Information and Communication Technologies for Ageing Well and E-Health, 736 (2017), pp. 100–118. https://doi.org/10.1007/978-3-319-62704-5_7.

[8] R. Igual, C. Medrano, and I. Plaza, *Challenges, Issues and Trends in Fall Detection Systems*, Biomedical Engineering Online, 12 (2013), p. 66, https://doi.org/10.1186/1475-925X-12-66.

[9] S. Junnila, A. Akhbardeh, and A. Värri, *An Electromechanical Film Sensor Based Wireless Ballistocardiographic Chair: Implementation and Performance*, Journal of Signal Processing Systems, 57 (2009), pp. 305–320, https://doi.org/10.1007/s11265-008-0307-2.

[10] F. Korbinian, M. J. V. Nadales, P. Robertson, and T. Pfeifer, *Bayesian Recognition of Motion Related Activities with Inertial Sensors*, in ACM International Conference on Ubiquitous Computing, 2010, pp. 445–446. https://doi.org/10.1145/1864431.1864480.

[11] B. Kwolek and M. Kepski, *Human Fall Detection on Embedded Platform Using Depth Maps and Wireless Accelerometer*, Computer Methods and Programs in Biomedicine, 117 (2014), pp. 489–501, https://doi.org/10.1016/j.cmpb.2014.09.005.

[12] S. R. Lord, C. Sherrington, H. B. Menz, and J. C. T. Close, *Falls in Older People: Risk Factors and Strategies for Prevention*, Cambridge University Press, 2 ed., 2007. ISBN 9781108706087.

[13] X. Ma, H. Wang, B. Xue, M. Zhou, B. Ji, and Y. Li, *Depth-Based Human Fall Detection Via Shape Features and Improved Extreme Learning Machine*, IEEE Journal of Biomedical and Health Informatics, 18 (2014), pp. 1915–1922, https://doi.org/10.1109/JBHI.2014.2304357.

[14] L. Martínez-Villaseñor, H. Ponce, J. Brieva, E. Moya-Albor, J. Núñez-Martínez, and C. Peñafort-Asturiano, *UP-Fall Detection Dataset: a Multimodal Approach*, Sensors, 19 (2019), p. 1988, https://doi.org/10.3390/s19091988.

[15] G. Mastorakis and D. Makris, *Fall Detection System Using Kinect's Infrared Sensor*, Journal of Real-Time Image Processing, 9 (2014), pp. 635–646. http://dx.doi.org/10.1007/s11554-012-0246-9.

[16] C. Medrano, R. Igual, I. Plaza, and M. Castro, *Detecting Falls as Novelties in Acceleration Patterns Acquired with Smartphones*, PLOS ONE, 9 (2014), pp. 1–9, https://doi.org/10.1371/journal.pone.0094811.

[17] L. Minvielle, M. Atiq, R. Serra, M. Mougeot, and N. Vayatis, *Fall Detection Using Smart Floor Sensor and Supervised Learning*, in International Conference of the IEEE Engineering in Medicine and Biology Society (EMBC), 2017, pp. 3445–3448, https://doi.org/10.1109/EMBC.2017.8037597.

[18] L. Montanini, A. Del Campo, D. Perla, S. Spinsante, and E. Gambi, *A Footwear-Based Methodology for Fall Detection*, IEEE Sensors Journal, 18 (2018), pp. 1233–1242, https://doi.org/10.1109/JSEN.2017.2778742.

[19] A. Mounir, P. Sergio, and M. Mougeot, *Constrained Prediction Time Random Forests Using Equivalent Trees and Genetic Programming: Application to Fall Detection Model Embedding*, in IEEE International Conference on Tools with Artificial Intelligence (ICTAI), 2021, pp. 690–697, https://doi.org/10.1109/ICTAI52525.2021.00109.

[20] F. Ofli, R. Chaudhry, G. Kurillo, R. Vidal, and R. Bajcsy, *Berkeley MHAD: a Comprehensive Multimodal Human Action Database*, in IEEE Workshop on Applications of Computer Vision (WACV), 2013, pp. 53–60, https://doi.org/10.1109/WACV.2013.6474999.

[21] M. Paajanen, J. Lekkala, and K. Kirjavainen, *ElectroMechanical Film (EMFi) - a New Multipurpose Electret Material*, Sensors and Actuators A: Physical, 84 (2000), pp. 95–102, https://doi.org/10.1016/S0924-4247(99)00269-1.

[22] N. Pannurat, S. Thiemjarus, and E. Nantajeewarawat, *Automatic Fall Monitoring: a Review*, Sensors, 14 (2014), pp. 12900–12936, https://doi.org/10.3390/s140712900.

[23] T. Reinvuo, M. Hannula, H. Sorvoja, E. Alasaarela, and R. Myllylä, *Measurement of Respiratory Rate with High-Resolution Accelerometer and EMFit Pressure Sensor*, IEEE Sensors Applications Symposium, (2006), pp. 192–195, https://doi.org/10.1109/sas.2006.1634270.

[24] L. Z. Rubenstein, *Falls in Older People: Epidemiology, Risk Factors and Strategies for Prevention*, Age and Ageing, 35 (2006), pp. 37–41, https://doi.org/10.1093/ageing/afl084.

[25] M. Saleh and R. Le Bouquin Jeannes, *FallAllD: a Comprehensive Dataset of Human Falls and Activities of Daily Living*, 2020, https://doi.org/10.21227/bnya-mn34.

[26] R. Serra, *Développement et Caractérisation D'un Système de Sol Piézoélectrique Intelligent. Application À la Détection des Chutes*, PhD thesis, Université de Strasbourg, 2017.

[27] A. Sucerquia, J. López, and J. Vargas-Bonilla, *SisFall: A Fall and Movement Dataset*, Sensors, 17 (2017), p. 198, https://doi.org/10.3390/s17010198.

[28] C. Truong, R. Barrois-Müller, T. Moreau, C. Provost, A. Vienne-Jumeau, A. Moreau, P.-P. Vidal, N. Vayatis, S. Buffat, A. Yelnik, D. Ricard, and L. Oudre, *A Data Set for the Study of Human Locomotion with Inertial Measurements Units*, Image Processing On Line, 9 (2019), pp. 381–390, https://doi.org/10.5201/ipol.2019.265.

[29] T. Vilarinho, B. Farshchian, D. G. Bajer, O. H. Dahl, I. Egge, S. S. Hegdal, A. Lønes, J. N. Slettevold, and S. M. Weggersen, *A Combined Smartphone and Smartwatch Fall Detection System*, in IEEE International Conference on Computer and Information Technology (CIT), 2015, pp. 1443–1448, https://doi.org/10.1109/CIT/IUCC/DASC/PICOM.2015.216.

[30] T. Xu, Y. Zhou, and J. Zhu, *New Advances and Challenges of Fall Detection Systems: A Survey*, Applied Sciences, 8 (2018), p. 418, https://doi.org/10.3390/app8030418.

[31] Z. Zhang, C. Conly, and V. Athitsos, *Evaluating Depth-Based Computer Vision Methods for Fall Detection Under Occlusions*, in International Symposium on Visual Computing, 2014, pp. 196–207, https://doi.org/10.1007/978-3-319-14364-4_19.